Biochimica et Biophysica Acta 1777 (2008) 532–539

Contents lists available at ScienceDirect

Biochimica et Biophysica Acta

journal homepage: www.elsevier.com/locate/bbabio

Hydrogencarbonate is not a tightly bound constituent of the water-oxidizing complex in photosystem II

Dmitriy Shevela [a,1], Ji-Hu Su [a], Vyacheslav Klimov [b], Johannes Messinger [a,*,1]

[a] Max-Planck-Institut für Bioanorganische Chemie, D 45470 Mülheim an der an Ruhr, Germany
[b] Institute of Basic Biological Problems, RAS, 142290 Pushchino, Moscow Region, Russia

ARTICLE INFO

Article history:
Received 15 February 2008
Received in revised form 17 March 2008
Accepted 18 March 2008
Available online 7 April 2008

Keywords:
Membrane-inlet mass spectrometry (MIMS)
Photosystem II
Water-splitting
Water oxidation
Hydrogencarbonate
Bicarbonate

ABSTRACT

Since the end of the 1950s hydrogencarbonate ('bicarbonate') is discussed as a possible cofactor of photosynthetic water-splitting, and in a recent X-ray crystallography model of photosystem II (PSII) it was displayed as a ligand of the Mn_4O_xCa cluster. Employing membrane-inlet mass spectrometry (MIMS) and isotope labelling we confirm the release of less than one (≈0.3) HCO_3^- per PSII upon addition of formate. The same amount of HCO_3^- release is observed upon formate addition to Mn-depleted PSII samples. This suggests that formate does not replace HCO_3^- from the donor side, but only from the non-heme iron at the acceptor side of PSII. The absence of a firmly bound HCO_3^- is corroborated by showing that a reductive destruction of the Mn_4O_xCa cluster inside the MIMS cell by NH_2OH addition does not lead to any CO_2/HCO_3^- release. We note that even after an essentially complete HCO_3^-/CO_2 removal from the sample medium by extensive degassing in the MIMS cell the PSII samples retain ≥75% of their initial flash-induced O_2-evolving capacity. We therefore conclude that HCO_3^- has only 'indirect' effects on water-splitting in PSII, possibly by being part of a proton relay network and/or by participating in assembly and stabilization of the water-oxidizing complex.

1. Introduction

Photosystem II (PSII) is a membrane-bound pigment-protein complex (see Fig. 1a) that catalyzes light-driven water-splitting into molecular oxygen and hydrogen equivalents (protons and electrons) [1]:

$$2H_2O \rightarrow O_2 + 4H^+ + 4e^-. \quad (1)$$

While organic cofactors such as chlorophylls, pheophytins and carotenoids are responsible for light harvesting, energy transfer, and/or charge separation in PSII [2], water-splitting is catalyzed by the inorganic cofactors manganese and calcium. These latter cations form, in a 4:1 stoichiometry, the μ-oxo bridged Mn_4O_xCa cluster ($x \geq 5$ signifies the number of μ-oxo bridges), which is the heart of the water-oxidizing complex (WOC) at the donor side of PSII (Fig. 1a) [3,4]. The Mn_4O_xCa cluster sequentially stores four oxidizing equivalents (S_i states; $i = 0, 1, 2, 3, 4$ stored oxidizing equivalents) [5] that are created in the successive charge separation events in the PSII reaction center. After attaining the S_4 state molecular oxygen is formed and the released O_2 is replaced by two unequivalently bound substrate water molecules (for review see [6–8]).

Another indispensible cation for PSII is iron [4,9]. On the acceptor side a non-heme iron is bound to the D1 and D2 proteins in the center between the two plastoquinone electron-acceptor molecules Q_A and Q_B (Fig. 1a, b) [10]. In addition, one heme iron is part of the cytochrome *b*559 subunit, which is assumed to be a component of the photoprotection network of the primary electron donor P680 (Fig. 1a) [11–13]. Cyanobacetria contain a second heme iron in the extrinsic c550 protein at the donor side of PSII (Fig. 1a) (reviewed in [14]).

Two anions are also discussed as cofactors of PSII: chloride (Cl^-) and hydrogencarbonate (HCO_3^-; also referred to as 'bicarbonate') [15,16]. Cl^- is either assumed to be a ligand to the Mn_4O_xCa cluster or to be part of the H-bonding network of the WOC that tunes the energetics of the redox (S_i state) transitions of the Mn_4O_xCa cluster [17,18].

Since the 1970s both the donor and acceptor sides of PSII are considered as possible binding sites for HCO_3^- (Fig. 1a, b, c; reviewed in [16,19,20]). Binding of HCO_3^- at the acceptor side of PSII as a ligand of the non-heme iron [21–23] was recently supported by two PSII crystal structures (Fig. 1b; [4,9]). Replacement of HCO_3^- at this site by its chemical analogs formate (HCO_2^-) or acetate ($CH_3CO_2^-$) is reported to slow down the Q_A^- to Q_B electron transfer and to thereby inhibit PSII [24–26]. This acceptor side effect complicates the search for specific effects of HCO_3^- on the donor side of PSII. Hence, several different options are currently discussed [16]: 1) exchangeable HCO_3^- delivers substrate water to the WOC, 2) HCO_3^- is a (loosely bound) part of the proton relay network of the WOC, 3) HCO_3^- plays an important role

* Corresponding author. Fax: +49 208 306 3951.
E-mail address: messinger@mpi-muelheim.mpg.de (J. Messinger).
[1] Future address: Department of Chemistry, Umeå University, S- 901 87 Umeå, Sweden.

0005-2728/$ – see front matter © 2008 Elsevier B.V. All rights reserved.
doi:10.1016/j.bbabio.2008.03.031

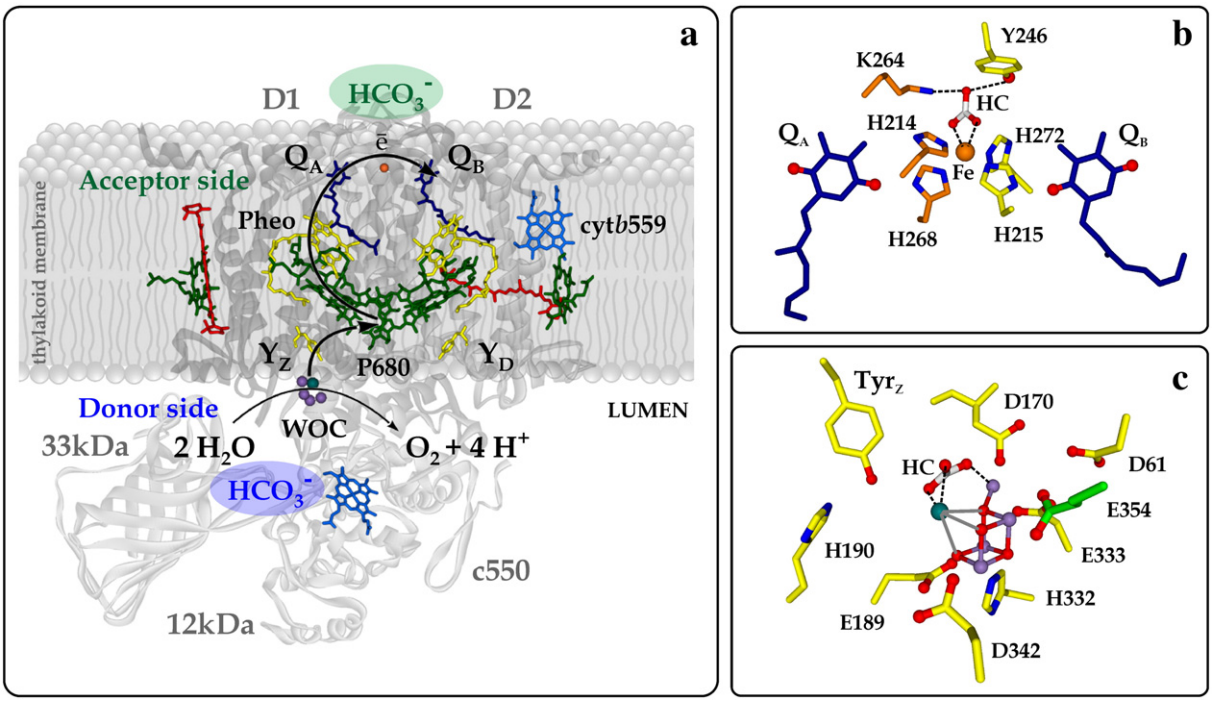

Fig. 1. Panel a shows a schematic view of the photosystem II (PSII) complex in the thylakoid membrane that is based on the 3.0 Å crystal structure of Loll et al. [4]. The core proteins of PSII are shown in gray with corresponding labels. The cofactors of the D1, D2, Cyt *c*550, and Cyt *b*559 proteins are placed in color on top of the proteins (see text for more details). Panel b presents a stereoview of the HCO_3^- binding site at the acceptor side of PSII, while Panel c displays a stereoview of possible HCO_3^- binding site within the WOC (donor side of PSII). The structures shown in Panels b and c were derived from the 3.5 Å crystal structure of Ferreira et al. [9]. Mn ions are shown in magenta; oxygen's in red, Fe in orange, and Ca, in green.

during photoactivation, but is not part of the WOC and 4) HCO_3^- is a (tightly bound) constituent of the functional Mn_4O_xCa cluster.

In recent studies we and others excluded option 1 [27,28]. We also showed that in higher plant (spinach) PSII 5-fold depletions of the CO_2 concentration in the buffer do not lead to significant changes in flash-induced oxygen evolution patterns [29]. However, these previous reports do not exclude the possibility that HCO_3^- is a tightly bound constituent of the WOC, which is essentially non-exchangeable [30,31]. This latter possibility is considered because HCO_3^- was shown to greatly accelerate the light-induced assembly of the Mn_4O_xCa cluster [16,32–34]. Further support for this idea comes from findings that formate and acetate also bind at the donor sides of PSII, suggesting that they may replace the structurally similar HCO_3^- from its binding sites in the WOC (for recent reports see [35–39]), and from recent X-ray structure of the PSII core complex of *T. elongatus* [9] in which one HCO_3^- molecule was tentatively modelled as a non-protein ligand to the Mn_4O_xCa cluster. However, the latter assignment was questioned in a subsequent X-ray crystallography study of PSII [4].

A general problem with most studies concerning the HCO_3^- effects is that they do not monitor the amount of inorganic carbon C_i (H_2CO_3, HCO_3^-, CO_3^{2-}) that is (*i*) in the aqueous buffers, (*ii*) bound to PSII, and (*iii*) released upon formate or other additions. Currently only three controversial studies exist on the formate-induced CO_2 release: Govindjee et al. found a slow release of CO_2 after formate addition into spinach, maize and pea thylakoid membrane or chloroplast suspensions [40,41], while Stemler did not find evidence for formate-induced release of CO_2 with maize chloroplasts [42,43]. In this study we employ membrane-inlet mass spectrometry to specifically probe and quantify the binding of C_i to the acceptor and donor sides of spinach PSII membranes. To accelerate the equilibration between C_i and the measured CO_2 carbonic anhydrase (CA) is added to the medium. A preliminary account of part these findings is given in the PS07 (Glasgow) conference proceedings [44].

2. Materials and methods

2.1. Sample preparation

PSII membranes, 'BBY' *type*, were prepared from fresh spinach leaves as described earlier [45,46]. The samples were then resuspended to a chlorophyll (Chl) concentration of ~6 mM in 50 mM MES buffer (pH 6.0), containing 400 mM sucrose, 15 mM NaCl, 5 mM $MgCl_2$, and 5 mM $CaCl_2$ and stored as liquid nitrogen droplets at −80 °C until used. Typical rates of oxygen evolution of studied samples were between 360 and 500 μmol O_2 (mg Chl)$^{-1}$ ml^{-1} h^{-1}. Before the measurements PSII samples were thawed in the dark on ice and diluted to the desired concentrations with MCMM buffer (400 mM mannitol, 20 mM $CaCl_2$, 10 mM $MgCl_2$, and 100 mM MES/NaOH) at pH 6.3–6.4.

2.2. Chemicals

$H_2^{18}O$ (98.5% enrichment) and $^{15}NH_2OH{\cdot}HCl$ (with assay of ^{15}N atom ≥98.0%) were purchased from Isotec.

2.3. Depletion of C_i

If not stated otherwise, all solutions were depleted of C_i by intensive flushing with argon in septum sealed vials for 10–20 min. In line with our previous report [29], such C_i-depletion procedure leads to an about 50-fold reduction of C_i-levels in the medium. To avoid CO_2 contamination when handling samples, all transfers into MIMS cell were made with gas tight syringes that had been pre-flushed with argon.

2.4. Mn-depletion from the WOCs

Hydroxylamine treatment/injection of PSII samples was performed either (*i*) in 1.5-ml Eppendorf tubes [29] (for O_2 activity assays and Mn^{2+} EPR six line measurements) or (*ii*) directly inside of the MIMS cell. In the first case, PSII samples (2 mM Chl) were incubated with 7.5 mM NH_2OH (final concentrations) for 15 min in the dark on ice and then washed three times in NH_2OH-free MCMM medium (pH 6.3). For EPR measurements the pellets of the NH_2OH-treated PSII samples were then diluted to a Chl concentration of ~5.5 mM with MCMM buffer and loaded into 4 mm X-band EPR tubes. The samples were stored in liquid nitrogen until used. For O_2 assays the pellet was diluted to 1 mM Chl in MCMM buffer and then studied as described below (Section 2.5). For MIMS measurements, the 150-μl MIMS cell was filled with PSII membranes and NH_2OH (7.5 mM final concentration) was injected into the cell after 25 min of degassation. The final Chl concentration of the PSII membranes in the MIMS cell after

10-μl injection of NH_2OH was 2 mM. All hydroxylamine additions were made from freshly prepared and pH adjusted $NH_2OH{\cdot}HCl$ stock solutions (120 mM, pH 6.3–6.4, 20 °C) in MCMM buffer. This concentration was shown to be sufficient for full extraction of all Mn from PSII (see Results section) and not to affect the CO_2 determination.

Hydrazine treatment was carried out based on a method described in [47] with some changes. Thawed PSII membrane fragments (6 mM Chl) were diluted to 2.25 mM Chl with a freshly prepared NH_2NH_2 stock solution in MCMM buffer (120 mM NH_2NH_2, pH 6.3 adjusted at 20 °C) and incubated for 30 min in the dark on ice. These samples were then directly transferred (without washing) into the MIMS cell, and further additions of (*i*) 10 μl of the NH_2NH_2 stock solution, (*ii*) 5-μl carbonic anhydrase (CA) solution and (*iii*) 5-μl $H_2^{18}O$ were made. The final chlorophyll concentration in the cell was 2.0 mM, and the final NH_2NH_2 concentration was ≈80 mM. The samples were then further incubated in the MIMS cell at 20 °C for 45 min in order to reach a baseline with a sufficiently low slope. Our NH_2NH_2 treatment resulted in a complete suppression of the O_2 evolution activity of the samples (checked by Joliot-type measurements) and in a complete extraction of the Mn from the WOC (checked by EPR measurements).

Heat treatment of PSII membrane was performed in EPR tubes by a 20-min dark-incubation in a 55–60 °C hot water bath according to the method described in [48].

HCl treatment was done according to [49] with slight modifications. HCl was added to PSII samples ([Chl] ≈ 4–5 mM) directly in EPR tubes to give a final HCl concentration of 0.3–0.5 M.

2.5. O_2 evolution activity assays

Rates of O_2 evolution of PSII membranes (20 mM Chl) were measured using a Clark-type electrode at 25 °C under continuous actinic illumination. 200 μM of phenyl-*p*-benzoquinone (PPBQ) and 500 μM $K_3[Fe(CN)_6]$ were used as electron acceptors during the measurements. In some cases also flash-induced oxygen evolution patterns were measured with our Joliot-type electrode as described in [29,50]. O_2 evolution activity measurements of PSII membranes performed within the MIMS cell are described in the Results section (see also legend of Fig. 2).

2.6. CW-EPR measurements (Mn determination)

CW-EPR measurements were performed using a *Bruker ELEXSYS E500* X-band spectrometer with the *Bruker* standard cavity ST4102. An *Oxford 900* liquid helium cryostat and the *ITC-503* temperature controller (*Oxford Instruments Ltd.*) were used to regulate the sample temperature to 7.0 K. Other instrumental conditions are given in the figure legends.

2.7. Membrane-inlet mass spectrometry (MIMS)

MIMS measurements (for review see [51]) were performed with an isotope ratio mass spectrometer (*ThermoFinnigan^{Plus} XP*) that was connected *via* a cooling trap (dry ice+ethanol) to a 150-μl home-built sample chamber (MIMS cell; similar to that described by Messinger et al. [52]). The sample in the MIMS cell was separated from the vacuum (3×10^{-8} bar) of the mass spectrometer by a silicon membrane (*Mempro MEM-213*) resting on a porous plastic support. After filling the chamber with the PSII sample, $H_2^{18}O$ was injected to give a final ^{18}O-enrichment of 3%, 6% or 65%. In order to facilitate equilibration between CO_2 and HCO_3^-, carbonic anhydrase (*CA; Sigma C3934*, from bovine erythrocytes, 2699 W-A U/mg protein) was added to the PSII samples before measurements to a final concentration of 3 μg ml^{-1} (experiments without CA required significantly longer degassation times, but yielded for all tested cases similar results). Depending on the ^{18}O-enrichment level in the MIMS cell, the samples were degassed for 30–100 min before the measurements until an only slightly sloping baseline was reached. Except for the CO_2 calibration experiments, all injections performed during the measurements were done with thoroughly C_i-depleted solutions (see above) using gas tight syringes.

3. Results

3.1. Activity of PSII samples in the MIMS cell during CO_2-depletion by degassation

Our stirred membrane-inlet mass spectrometry (MIMS) cell has a volume of 150 μl and is connected to the vacuum of the isotope ratio mass spectrometer *via* a 1 cm diameter inlet that is covered by a 25 μm thick silicon membrane resting on a porous plastic support [52]. This arrangement leads to a fast degassing of the PSII suspensions in the MIMS cell and hence allows probing the effects of HCO_3^- depletion of the buffer on the activity of PSII *via* simultaneous monitoring of the O_2 and CO_2 signals at mass to charge ratios of 32, 34, 36 and 44, 46 and 48, respectively. Rapid equilibration between dissolved CO_2 and H_2CO_3, HCO_3^- and CO_3^{2-} (collectively referred to as C_i) occurs in the buffer due to the intrinsic carbonic anhydrase (CA) activity of PSII [53,54], which is further enhanced by the addition of bovine CA. For better S/N these experiments were performed with an $H_2^{18}O$ enrichment of 3% (Fig. 2a) or 6% (Fig. 2b).

The grey line in Fig. 2a shows the relative CO_2 concentration of the PSII suspension (0.4 mM Chl final, 1.5 mM $K_3[Fe(CN)_6]$) that was measured at $m/z=46$ ($^{12}C^{16}O^{18}O$). After about 40 min an essentially complete removal (>40 times depletion compared to air saturation; please note that for technical reasons the first 140 s after sample filling could not be recorded) of CO_2 (and all other gases) from the medium is achieved. During this degassing the water-splitting activity of PSII was probed by illuminating the sample every 5 to 10 min with trains of 10 saturating Xe-flashes (2 Hz frequency). The resulting O_2-evolution was detected at $m/z=34$ ($^{16}O^{18}O$) and is displayed in Fig. 2a as black line. A visual inspection of Fig. 2a indicates that the oxygen evolving activity of PSII decreases only slightly despite the sharp drop in the concentration of dissolved CO_2. Fig. 2b displays the results of a similar experiment on a longer time course in which the samples were given 10 flashes (2 Hz) every 20 to 40 min. The black squares in Fig. 2b give the integrated O_2-yields that are normalized to the extrapolated value at the time of injection into the MIMS cell. An inspection reveals that the PSII membranes lose about 20% of their initial flash-induced O_2-

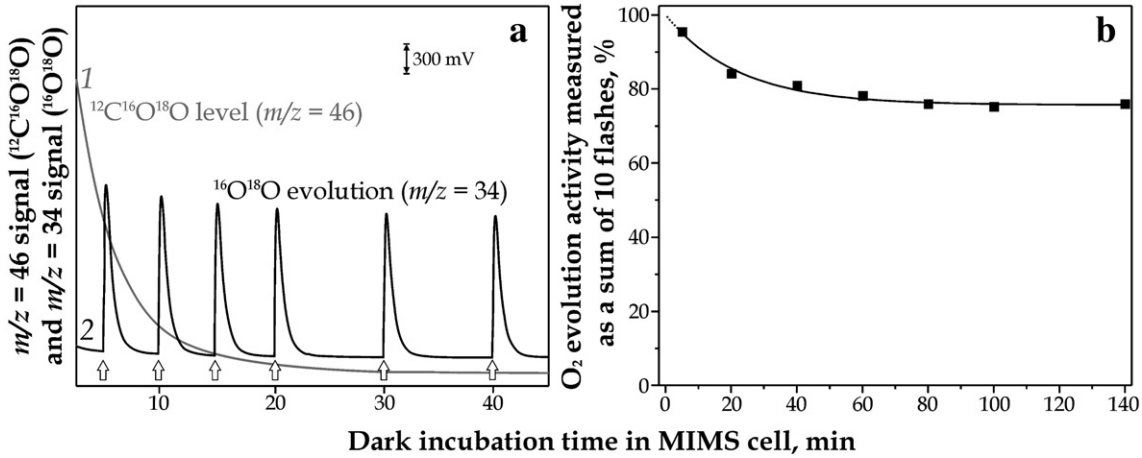

Fig. 2. a, Level of $^{12}C^{16}O^{18}O$ ($m/z=46$; *1*, grey trace) and O_2 yields induced by a series of 10 saturating Xe flashes (2 Hz) measured at $^{16}O^{18}O$ ($m/z=46$; *2*, black trace) as a function of degassation time of PSII membrane fragments in the MIMS cell at pH 6.3 and 20 °C. The $H_2^{18}O$ enrichment was 3%. The onsets of flash illuminations are marked by arrows. b, same as a, but with an $H_2^{18}O$ enrichment of 6%. Squares represent the integrated and normalized (to projected value at the time of injection) $m/z=34$ ($^{16}O^{18}O$) signal intensities that were induced by 10 saturating Xe flashes as described above. All measurements were carried out with a Chl concentration of 0.4 mg ml^{-1} in the presence of 1.5 mM $K_3[Fe(CN)_6]$ as electron acceptor and [CA] = 3 μg ml^{-1}.

evolving capacity during the first 40 min of degassing. Only a very small further drop (by about 5%) is seen at times up to 2 h. While there appears to be a qualitative correlation between loss in activity and the declining CO_2/HCO_3^- level, there is clearly no direct (1:1) correlation, since the samples retain ≥75% activity even after prolonged incubation in essentially C_i-free buffer (pH 6.3).

3.2. Formate-induced release of C_i from PSII

Fig. 3 shows that the injection of a few μl of a concentrated (100 mM final concentration in MIMS cell), argon bubbled (to remove C_i) formate solution leads to the slow liberation of CO_2 from untreated spinach PSII membranes (trace 1; 3% $H_2^{18}O$). The observed CO_2 release (shown here is only the m/z=46 signal) is significantly larger than the small artifact that is observed upon injection of formate solution into the buffer (trace 4), and it is also proportional to the sample concentration (data not shown, but see [44]). A second addition of 100 mM formate into already treated PSII samples gives a practically identical response to the injection into buffer (compare traces 3 and 4, Fig. 3). This indicates that 100 mM formate (final concentration) is sufficient to release all HCO_3^- from PSII that is replaceable by formate at pH 6.3.

Since formate was reported to bind at both the acceptor and donor sides of PSII [36,37], the origin of the released C_i remains unclear. In order to allow discriminating between these two options the Mn_4O_xCa cluster was removed from the PSII samples by a 75-min incubation with 80 mM NH_2NH_2 prior to the injection of 100 mM formate (trace 2). This hydrazine treatment leads to a complete loss in O_2 activity (confirmed by Joliot-type measurements; data not shown) and to the release of all Mn from PSII (confirmed by EPR measurements; data not shown, but similar to Fig. 5). Comparison of traces 1 and 2 in Fig. 3 clearly shows that in both cases practically the same amount of CO_2 is released upon formate addition. The same CO_2 release was also observed for samples from which the released Mn and the remaining NH_2NH_2 were removed prior to the measurements by several washing steps (data not shown).

This indicates that C_i released upon formate addition does not originate from the WOC, but comes from a different binding site within PSII (see also [30]). According to the literature this binding site is at the non-heme iron of the acceptor side.

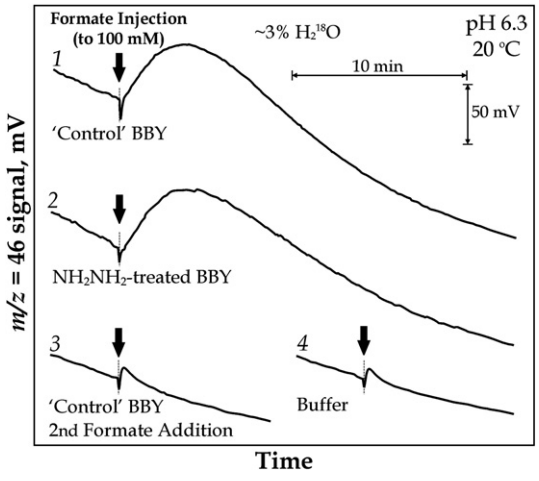

Fig. 3. C_i release upon formate addition (100 mM final) to: non-treated 'control' BBY particles (trace 1), BBY particles pre-incubated with 80 mM NH_2NH_2 for 75 min to release all Mn from the WOC (trace 2), formate pre-treated BBY (trace 3) and buffer (trace 4). C_i was detected at as $^{12}C^{16}O^{18}O$ at m/z=46 with MIMS. Before the injections of argon bubbled formate stock solutions (marked by closed arrows) all samples were thoroughly degassed in the MIMS cell for 45 min. Other conditions: pH 6.3; 20 °C; 3% $H_2^{18}O$ enrichment; [CA] = 3 μg ml^{-1}; final chlorophyll concentration was 2 mg ml^{-1}. For all cases one representative result out of 2–4 repeat measurements is presented.

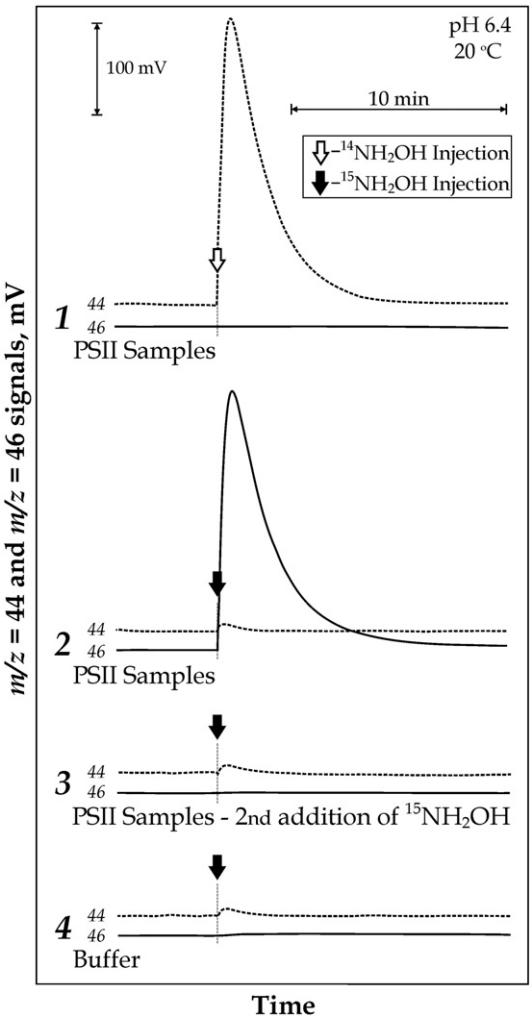

Fig. 4. MIMS measurements of N_2O evolution induced by the addition (arrows) of non-labelled NH_2OH (trace 1) and ^{15}N-labelled NH_2OH (trace 2) to PSII samples ([Chl] = 2 mg ml^{-1}) monitored at m/z=44 (dash traces) and m/z=46 (solid traces). Trace 3 displays the 2nd injection of ^{15}N-labelled NH_2OH into PSII samples (15 min after the 1st injection shown in trace 2), while the injection artifact caused by the addition of ^{15}N-labelled NH_2OH into the MCMM buffer (pH 6.4) presented in trace 4. Only C_i-depleted $^{15}NH_2OH/^{14}NH_2OH$ solutions were used for the 10-μl injections into the samples that were degassed for 25 min in the 150-μl MS cell prior to the above injections. The measurements were performed in the presence of CA (3 μg ml^{-1}) at pH 6.4 and 20 °C. The final NH_2OH concentrations were 7.5 mM.

3.3. Quantification of the released CO_2

For the quantification of the amount of CO_2 released by formate addition in Fig. 3 (traces 1 and 2) the injection artifact (trace 4) and the sloping baseline were subtracted. The signals were then quantified by integration within OriginPro software. A linear correlation between the amount of dissolved CO_2 (nmol) and signal area was established by injecting various amount of air-saturated water into the degassed buffer (3% $H_2^{18}O$ enrichment) in the MIMS cell. On this basis a formate-induced CO_2 release of 0.34±0.01 nmol C_i was calculated for traces 1 and 2 in Fig. 3 and for five repeat measurements at pH 6.3. Since the final Chl concentration in the above experiments was 2 mM, a ratio of approx. 0.3 CO_2/HCO_3^- per PSII reaction center (RC) can be calculated assuming 250 Chl/RC (1.2 nmol RC in 150 μl). This ratio is very similar to results obtained earlier by Govindjee et al. [40,41], where for spinach thylakoids a ratio of 0.4 HCO_3^-/CO_2 per reaction center was determined by mass spectrometry. Ratios of 0.5–1.2 C_i/RC were reported by the same authors for maize and pea thylakoids employing an infrared gas analyzer [41], while Stemler was unable to detect a formate-induced CO_2 release in maize thylakoids [42,43].

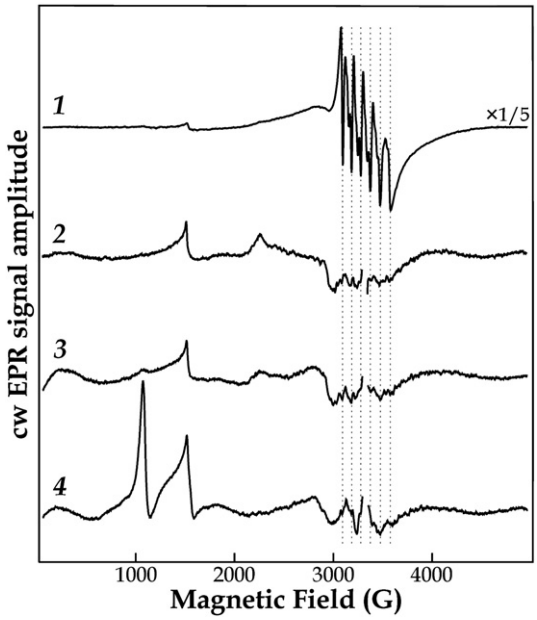

Fig. 5. cw-EPR spectra of BBY samples ([Chl]=5.5 mg ml^{-1}) at 7 K: spectrum *1*, dark adapted samples after 20-min heat treatment in water bath at 57 °C; spectrum *2*, samples that were incubated for 15 min with 7.5 mM NH_2OH on ice at pH 6.3 and then washed three times in NH_2OH-free MCMM medium (pH 6.3); spectrum *3*, same sample as in spectrum *2*, but after an additional 20-min heat treatment in water bath at 57 °C; spectrum *4*, same sample as before (spectra *2* and *3*), but after addition of approx. 0.3 M HCl (final concentration). EPR settings: microwave frequency, 9.41 GHz; microwave power, 20 mW; modulation amplitude, 15.0 G; modulation frequency, 100 kHz. Each spectrum is the average of 8 scans.

3.4. Is HCO_3^- an integral part of the WOC?

The above experiments (Section 3.2) show that formate is unable to displace HCO_3^- from the WOC. However, due to the arguments mentioned in the Introduction it may still be speculated that HCO_3^- is an integral, non-formate-displaceable constituent of the intact WOC. This possibility can be probed by destroying the Mn_4O_xCa cluster inside the MIMS chamber by small additions of highly concentrated, pH adjusted and argon bubbled NH_2OH solutions. The idea behind this approach is that even a buried, firmly bound C_i molecule will be released into the medium upon the complete reductive removal of the Mn_4O_xCa cluster from the WOC, because of the several orders of magnitude lower binding affinity of HCO_3^- to $Mn^{2+}$and Ca^{2+}, compared to HCO_3^- binding to Mn^{3+}/Mn^{4+} present in the intact WOC [55]. The main differences to the above experiment (Fig. 3, trace 2) are *i*) that the m/z=46 signal is now monitored during the injection and incubation with the reductant, and *ii*) that no formate is employed.

Injection of 7.5 mM (final concentration) $^{14}NH_2OH$ into a suspension of intact PSII membranes (no $H_2^{18}O$ enrichment) leads to strong signals at m/z=44 (trace 1 in Fig. 4), which are clearly above the injection artifacts (not shown, but see trace 4 in Fig. 4 for $^{15}NH_2OH$ injection into buffer). No signal is seen at this amplification for m/z=46, since this experiment was performed without $H_2^{18}O$ enrichment. The m/z=44 signal (experiment 1 in Fig. 4) is proportional to the PSII concentration (data not shown) and second injections of NH_2OH lead to signals that equal the injection into buffer (not shown, but similar to traces 3 and 4; Fig. 4). The latter finding indicates that the applied NH_2OH concentration is sufficient to completely reduce and release the Mn from the WOC. This was confirmed for parallel samples by *i*) Clark-type O_2 measurements that show no traces of light-induced O_2 evolution (data not shown), and *ii*) by EPR measurements documenting that no further Mn could be released from such NH_2OH treated samples by heating to 57 °C for 20 min or by addition of 0.3 M HCl (Fig. 5, traces 2–4). Trace 1 of Fig. 5 displays for comparison the Mn^{2+} EPR six line signal that is observed after heat treatment of a control PSII sample.

Table 1
Relative theoretical molecular distribution of natural isotopes of CO_2 and N_2O compared to experimental isotope distribution of the gas released by $^{14}NH_2OH$ injection into PSII suspensions (see Fig. 4, trace 1)

	Theoretical (%)[a]		Experimental (%)[b]
m/z	CO_2	N_2O	$^{14}NH_2OH$ injection
44	99.60	99.80	99.80±0.02
46	0.40	0.20	0.20±0.02

[a] Isotopic distributions of the molecules were calculated using on-line Molecular Isotopic Distribution Calculator Program (http://www2.sisweb.com/mstools/isotope.htm). Mass 48 is not taken into account since our MIMS measurements were done without ^{18}O enrichment (see Fig. 4).
[b] The values were obtained by subtracting the injection artifact and subsequent signal integration. Values are the mean of three independent measurements.

At first glance these data appear to suggest that the destruction of the WOC indeed leads to the liberation of C_i into the medium, which then can be detected as CO_2 at m/z=44. However, another gas, N_2O, has approximately the same molecular mass as CO_2 and has been previously reported to be formed (in addition to N_2) during the reaction of hydroxylamine with the WOC [56]. The reaction sequence of NH_2OH with the WOC is not fully analyzed but can be represented by:

$$4\,NH_2OH + WOC(2Mn^{3+}/2Mn^{4+}) \rightarrow N_2O + N_2 + 4\,Mn^{2+}_{(free)} + 3\,H_2O + 6\,H^+. \quad (2)$$

Studies of the kinetics of the NH_2OH oxidation by Mn^{III}-complexes *in vitro* also showed that the most common oxidation products of NH_2OH are N_2O and N_2 [57,58].

A close inspection of the isotope ratios of the m/z 44 and 46 signals (Table 1) indicates that the released gas is N_2O rather than CO_2. This was confirmed by injections of $^{15}NH_2OH$ into PSII suspensions. Trace 2 in Fig. 4 clearly displays the expected shift of the m/z=44 signal by two mass units to m/z=46. This shift does not disclose any m/z=44 signal that is above the injection artifact. However, since the m/z=44 peak is less sensitive in our setup we confirmed this result by measurements at m/z=48, for which we employed an $H_2^{18}O$ enrichment for the buffer of 65% and injections but unlabelled ($^{14}NH_2OH$). The idea behind this

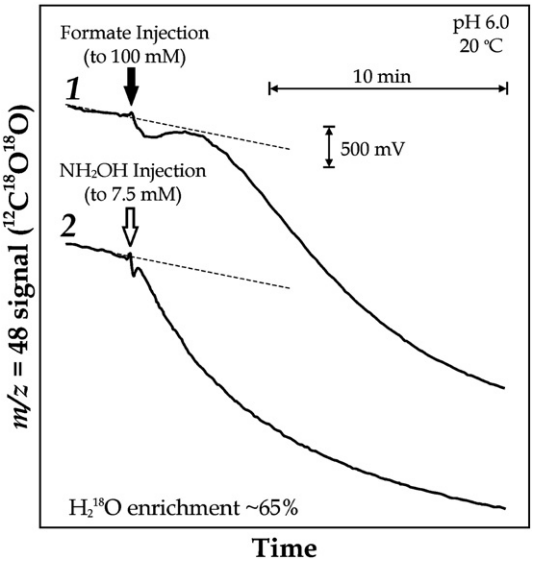

Fig. 6. Formate-induced release of CO_2 (trace 1) compared with the absence of CO_2 release upon the injection of NH_2OH (trace 2) measured by MIMS at m/z=48 in spinach PSII membranes ([Chl]=2 mg ml^{-1}) at pH 6.0 and 20 °C. Prior to the 10-μl injections of C_i-depleted formate (final concentration 100 mM) or C_i-depleted $^{14}NH_2OH$ (final concentration 7.5 mM) the PSII samples were degassed in the MS cell for 100 min to reach a sufficiently low slope of the baseline. The measurements were performed in the presence of carbonic anhydrase [CA]=3 μg ml^{-1} at an $H_2^{18}O$ enrichment of approx. 65%.

experiment is that among the two species of interest only CO_2 ($^{12}C^{18}O^{18}O$), and not $^{14}N_2O$ can give rise to a signal at m/z=48. Fig. 6, trace 1 shows that the injection of 100 mM formate leads to a clearly detectable CO_2 release in agreement with the above described data (compare to Fig. 3). It should be noted that the employed formate solution (and below the NH_2OH solution) was not enriched with $H_2^{18}O$ water. Therefore, the formate-induced CO_2 release from PSII is observed on top of a negative baseline shift that reflects the CA catalyzed isotopic equilibration between water and CO_2 after the small reduction of the $H_2^{18}O$ enrichment caused by the formate injection. Trace 1 is shown as proof that the chosen conditions are sensitive enough to detect the release of about ≤0.3 HCO_3^- per PSII. Trace 2 of Fig. 6 shows that the injection of NH_2OH does not lead to any CO_2 formation from PSII, because only the above described baseline shift is observed. Taken together, the above data provide strong evidence against the presence of a tightly bound C_i in the WOC. It is worth noting that the same conclusion was reached in a GC-MS study that appeared on-line on the day of submission of this work [59].

4. Discussion

4.1. HCO_3^- interactions at the acceptor side

Our data clearly confirm that HCO_3^- can be released from PSII by the addition of formate. On the basis of literature data the most probable binding site for this HCO_3^- anion is the non-heme iron at the acceptor side. The substoichiometric amount of about 0.3 HCO_3^- per PSII may at least in part be explained by the loss of some bound HCO_3^- into the medium during the required 40-min degassing in the MIMS cell. However, similar ratios (0.4 to 1.2) were previously reported by Govindjee et al. using different approaches [40,41]. Therefore, the occupancy of non-heme iron binding site by HCO_3^- in undepleted buffer remains to be established.

Since we were unable to determine the amount of bound HCO_3^- at shorter degassing times, it is difficult to establish a clear correlation between the 20–25% loss in flash-induced O_2 evolution activity and the pronounced decline in the C_i content of the buffer. However, it was previously suggested that HCO_3^- binding at the non-heme iron is important for a fast protonation of Q_B^{2-}, and that a slowing of this reaction may become rate limiting for O_2 production [60,61]. In flashing light (2 Hz) such a rate limitation is naturally less significant for the overall O_2 yield as compared to continuous illumination. Therefore, our data may be in agreement with the above idea. However, at present it also appears possible that the effects of easily removable HCO_3^- on the donor side (discussed below), or factors unrelated to the HCO_3^- concentration are responsible for the activity loss. In any case, it is remarkable, that the samples remain highly active (~75–80%) even after prolonged (greater than 2 h) degassing (Fig. 2). These data show that neither dissolved CO_2/HCO_3^- nor e.g. O_2 is strictly required for water-splitting by PSII, but that they may only indirectly tune the overall activity of PSII by removing rate limitations that are possibly connected with protonation or deprotonation reactions.

4.2. HCO_3^- interactions at the donor side

Our membrane-inlet mass spectrometry data clearly demonstrate that neither formate addition nor the reductive destruction of the Mn_4O_xCa cluster by NH_2OH liberate any HCO_3^- from the WOC. This is in line with a very recent FTIR study [62] that detected no HCO_3^- bands from the WOC in S_i state FTIR difference spectra. This strongly suggests that HCO_3^- is not a ligand of the Mn_4O_xCa cluster nor a cofactor strongly coupled to the Mn_4O_xCa cluster for example *via* substrate water. However, the elegant FTIR study left open the possibilities that *i*) HCO_3^- is an integral part of the WOC that cannot be isotopically labelled by the applied $H^{12}CO_3^-/H^{13}CO_3^-$ exchange treatment, *ii*) HCO_3^- binds to a Mn that is not affected by the oxidation state and structural changes during S_i state cycling and *iii*) HCO_3^- binds to a part of the protein pocket of the WOC that is unaffected by the S_i state transitions. Since our approach does neither rely on the exchangeability of the potentially tightly bound HCO_3^-, nor on its vibrational coupling to the S_i state dependent changes of the Mn_4O_xCa cluster, our results also fully exclude these remaining options. Therefore binding of HCO_3^- to WOC as displayed in Fig. 1c can be ruled out. However, HCO_3^- may be a transient Mn-ligand during the assembly of the Mn_4O_xCa cluster and/or stabilize the WOC indirectly during heat-stress by binding to other donor side components [34,63,64].

The presence of a weakly bound, rapidly exchanging HCO_3^- can, however, not be fully excluded by the presented experiments, since in that case all HCO_3^- may have been removed during the degassing prior to NH_2OH addition. In analogy to its proposed acceptor side function, such a 'mobile' or weakly bound HCO_3^- may be involved in the proton relay network of the WOC (see below). However, as discussed above, the data of Fig. 2 and our previous flash-induced oxygen evolution measurements with a Joliot-type electrode [29] indicate that removal of such a HCO_3^- has, under flashing light, only minor consequences on the activity of PSII.

4.3. Carbonic anhydrase activity of PSII

PSII from higher plants, cyanobacteria and green algae is known to posses an intrinsic carbonic anhydrase (CA) activity [27,53,54,65–68]. However, so far only in case of *Chlamydomonas* a specific CA, Cah3, was identified [69]. Shutova et al. suggested recently on the basis of detailed experiments with this mutant that the Cah3 protein, in the presence of its substrate HCO_3^-, plays an important role in proton translocation in the WOC [70]. Interestingly, the addition of bovine CA resulted in a significantly smaller stimulation. At present it is unclear whether a similar intrinsic CA/HCO_3^- effect exists in higher plant (spinach PSII membrane) preparations that were used in this study.

4.4. Formate

Formate (and to a lesser extend acetate) addition to PSII has strong effects on the overall flash-induced O_2 yields and the miss parameter during water-splitting ([29] and references therein). This is in striking contrast to the comparatively small effects of CO_2/HCO_3^- depletion. The present data therefore support the earlier suggested idea [29,42] that the effects of this anion should no longer be viewed as being mainly due to the displacement of a functionally important HCO_3^-, but as being due to its own inhibitory action on the acceptor and/or the donor sides of PSII.

5. Conclusion: role of hydrogencarbonate for the activity of photosystem II

It is well established that hydrogencarbonate plays an important role during the light-induced assembly of the Mn_4O_xCa cluster [32–34,39,71,72] by lowering the redox potential of the Mn^{2+}/Mn^{3+} pair [55], and that Mn^{2+}/HCO_3^- complexes may have been the original substrate during the evolution of today's PSII [73,74]. Nevertheless, the current study clearly demonstrates that in higher plants C_i is not a tightly bound constituent of the WOC. Given the fact that so far no major species differences have been found with regard to water-splitting, this finding most likely extends to PSII complexes from all other oxygenic organisms. The present data exclude several mechanistic ideas, including a recent one that invokes peroxydicarbonic acid as intermediate in water-splitting, because this would require two bound C_i molecules per WOC [75]. Since in addition a role of C_i as mobile substrate of PSII is excluded by this and previous studies [27,67,76], a direct involvement of C_i in water-splitting can now be ruled out.

Nevertheless, a regulatory function of HCO_3^- for PSII may be a desirable feed back mechanism with regard to CO_2 fixation, i.e. between the first and last components of the photosynthetic electron transport chain. This type of regulation may occur in a species dependent manner and may include HCO_3^- binding to the acceptor side [21] and/or the

involvement of HCO_3^- in the deprotonation reactions of the WOC [70]. Such interactions may explain a large part of the existing literature on the hydrogencarbonate (bicarbonate) effect. However, further studies, for example like the ones shown in Figs. 2 and 3 of this work, possibly combined with fluorescence measurements, will be required under various pH conditions and with several different organisms to further evaluate this possibility. Similarly, other indirect effects of C_i, like a stabilization of the PSII function at elevated temperatures [64,77] or the protection against photoinhibition [64], and a possible interaction between the two anions HCO_3^- and Cl^- [78] should be further characterized under flashing and continuous light.

Acknowledgements

The authors thank Katrin Beckmann for the help during the MIMS experiments, and Govindjee and Alan Stemler for their ongoing discussions about the 'bicarbonate effect'. We are also grateful to Gernot Renger and especially to Alan Stemler for critically reading the manuscript and several helpful suggestions. Financial support was provided by the Deutsche Forschungsgemeinschaft (DFG 1629/2-4) and the Max-Planck-Gesellschaft.

References

[1] T. Wydrzynski, K. Satoh (Eds.), Photosystem II. The Light-driven Water:Plastoquinone Oxidoreductase, Springer, Dordrecht, 2005.
[2] G. Renger, A.R. Holzwarth, Primary electron transfer, in: T.J. Wydrzynski, K. Satoh (Eds.), Photosystem II. The Light-driven Water:Plastoquinone Oxidoreductase, vol. 22, Springer, Dordrecht, 2005, pp. 139–175.
[3] J. Yano, J. Kern, K. Sauer, M.J. Latimer, Y. Pushkar, J. Biesiadka, B. Loll, W. Saenger, J. Messinger, A. Zouni, V.K. Yachandra, Where water is oxidized to dioxygen: structure of the photosynthetic Mn_4Ca cluster, Science 314 (2006) 821–825.
[4] B. Loll, J. Kern, W. Saenger, A. Zouni, J. Biesiadka, Towards complete cofactor arrangement in the 3.0 Å resolution structure of photosystem II, Nature 438 (2005) 1040–1044.
[5] B. Kok, B. Forbush, M. McGloin, Cooperation of charges in photosynthetic O_2 evolution, Photochem. Photobiol. 11 (1970) 457–476.
[6] W. Hillier, J. Messinger, Mechanism of photosynthetic oxygen production, in: T. Wydrzynski, K. Satoh (Eds.), Photosystem II. The Light-driven Water:Plastoquinone Oxidoredutase, vol. 22, Springer, Dordrecht, 2005, pp. 567–608.
[7] J. Messinger, G. Renger, Photosynthetic water splitting, in: G. Renger (Ed.), Primary Processes of Photosynthesis, Part 2 Principles and Apparatus, vol. 9, RSCPublishing, Cambridge, 2008, pp. 291–351.
[8] J.P. McEvoy, G.W. Brudvig, Water-splitting chemistry of photosystem II, Chem. Rev. 106 (2006) 4455–4483.
[9] K.N. Ferreira, T.M. Iverson, K. Maghlaoui, J. Barber, S. Iwata, Architecture of the photosynthetic oxygen-evolving center, Science 303 (2004) 1831–1838.
[10] V. Petrouleas, A.R. Crofts, The iron–quinone acceptor complex, in: T. Wydrzynski, K. Satoh (Eds.), Photosystem II. The Light-driven Water:Plastoquinone Oxidoreductase, vol. 22, Springer, Dordrecht, 2005, pp. 177–206.
[11] D.H. Stewart, G.W. Brudvig, Cytochrome *b*559 of photosystem II, Biochim. Biophys. Acta 1367 (1998) 63–87.
[12] P. Faller, A. Pascal, A.W. Rutherford, β-Carotene redox reactions in photosystem II: electron transfer pathway, Biochemistry 40 (2001) 6431–6440.
[13] O. Kaminskaya, V.A. Shuvalov, G. Renger, Evidence for a novel quinone-binding site in the photosystem II (PS II) complex that regulates the redox potential of cytochrome *b*559, Biochemistry 46 (2007) 1091–1105.
[14] J.L. Roose, K.M. Wegener, H.B. Pakrasi, The extrinsic proteins of photosystem II, Photosynth. Res. 92 (2007) 369–387.
[15] H.J. van Gorkom, C.F. Yocum, The calcium and chloride cofactors, in: T. Wydrzynski, K. Satoh (Eds.), Photosystem II. The Light-driven Water:Plastoquinone Oxidoreductase, vol. 22, Springer, Dordrecht, 2005, pp. 307–328.
[16] J.J.S. van Rensen, V.V. Klimov, Bicarbonate interactions, in: T. Wydrzynski, K. Satoh (Eds.), Photosystem II. The Light-driven Water:Plastoquinone Oxidoreductase, vol. 22, Springer, Dordrecht, 2005, pp. 329–346.
[17] H. Popelkova, C.F. Yocum, Current status of the role of Cl^- ion in the oxygen-evolving complex, Photosynth. Res. 93 (2007) 111–121.
[18] K. Olesen, L.-E. Andréasson, The function of the chloride ion in photosynthetic oxygen evolution, Biochemistry 42 (2003) 2025–2035.
[19] A.J. Stemler, The bicarbonate effect, oxygen evolution, and the shadow of Otto Warburg, Photosynth. Res. 73 (2002) 177–183.
[20] J.J.S. van Rensen, Role of bicarbonate at the acceptor side of photosystem II, Photosynth. Res. 73 (2002) 185–192.
[21] Govindjee, T. Wydrzynski, New site of bicarbonate effect in photosystem II of photosynthesis — evidence from chlorophyll fluorescence transients in spinach-chloroplasts, Biochim. Biophys. Acta 387 (1975) 403–408.
[22] Govindjee, M.P.J. Pulles, R. Govindjee, H.J. van Gorkom, L.N.M. Duysens, Inhibition of reoxidation of secondary-electron acceptor of photosystem II by bicarbonate depletion, Biochim. Biophys. Acta 449 (1976) 602–605.
[23] J.J.S. van Rensen, W.F.J. Vermaas, Action of bicarbonate and photosystem 2 inhibiting herbicides on electron-transport in pea grana and in thylakoids of a blue-green-alga, Physiol. Plant. 51 (1981) 106–110.
[24] Y. Deligiannakis, V. Petrouleas, B.A. Diner, Binding of carboxylate anions at the nonheme Fe(II) of PS II. 1. Effects on the $Q_A^-Fe^{2+}$ and Q_AFe^{3+} EPR spectra and the redox properties of the iron, Biochim. Biophys. Acta 1188 (1994) 260–270.
[25] A. Jajoo, S. Bharti, A. Kawamori, Interactions of chloride and formate at the donor and the acceptor side of photosystem II, J. Bioenerg. Biomembr. 37 (2005) 49–54.
[26] Govindjee, C.H. Xu, G. Schansker, J.J.S. van Rensen, Chloroacetates as inhibitors of Photosystem II: effects on electron acceptor side, J. Photochem. Photobiol. B Biol. 37 (1997) 107–117.
[27] J. Clausen, K. Beckmann, W. Junge, J. Messinger, Evidence that bicarbonate is not the substrate in photosynthetic oxygen evolution, Plant Physiol. 139 (2005) 1444–1450.
[28] W. Hillier, I. McConnell, M.R. Badger, A. Boussac, V.V. Klimov, G.C. Dismukes, T. Wydrzynski, Quantitative assessment of intrinsic carbonic anhydrase activity and the capacity for bicarbonate oxidation in photosystem II, Biochemistry 45 (2006) 2094–2102.
[29] D. Shevela, V. Klimov, J. Messinger, Interactions of photosystem II with bicarbonate, formate and acetate, Photosynth. Res. 94 (2007) 247–264.
[30] A. Stemler, Binding of bicarbonate ions to washed chloroplast grana, Biochim. Biophys. Acta 460 (1977) 511–522.
[31] A. Stemler, J. Murphy, Inhibition of HCO_3^--binding to photosystem II by atrazine at a low-affinity herbicide binding-site, Plant Physiol. 77 (1985) 179–182.
[32] V.V. Klimov, S.I. Allakhverdiev, Y.M. Feyziev, S.V. Baranov, Bicarbonate requirement for the donor side of photosystem II, FEBS Lett. 363 (1995) 251–255.
[33] V.V. Klimov, S.I. Allakhverdiev, S.V. Baranov, Y.M. Feyziev, Effects of bicarbonate and formate on the donor side of photosystem 2, Photosynth. Res. 46 (1995) 219–225.
[34] S.I. Allakhverdiev, I. Yruela, R. Picorel, V.V. Klimov, Bicarbonate is an essential constituent of the water-oxidizing complex of photosystem II, Proc. Natl. Acad. Sci. U. S. A. 94 (1997) 5050–5054.
[35] K.L. Clemens, D.A. Force, R.D. Britt, Acetate binding at the photosystem II oxygen evolving complex: an S2 state multiline signal ESEEM study, J. Am. Chem. Soc. 124 (2002) 10921–10933.
[36] Y.M. Feyziev, D. Yoneda, T. Yoshii, N. Katsuta, A. Kawamori, Y. Watanabe, Formate-induced inhibition of the water-oxidizing complex of photosystem II studied by EPR, Biochemistry 39 (2000) 3848–3855.
[37] A. Jajoo, N. Katsuta, A. Kawamori, An EPR study of the pH dependence of formate effects on Photosystem II, Plant Physiol. Biochem. 44 (2006) 186–192.
[38] H. Kühne, V.A. Szalai, G.W. Brudvig, Competitive binding of acetate and chloride in photosystem II, Biochemistry 38 (1999) 6604–6613.
[39] V.V. Klimov, R.J. Hulsebosch, S.I. Allakhverdiev, H. Wincencjusz, H.J. van Gorkom, A.J. Hoff, Bicarbonate may be required for ligation of manganese in the oxygen-evolving complex of photosystem II, Biochemistry 36 (1997) 16277–16281.
[40] Govindjee, H.G. Weger, D.H. Turpin, J.J.S. van Rensen, O.J. Devos, J.F.H. Snel, Formate releases carbon dioxide/bicarbonate from thylakoid membranes- measurements by mass spectroscopy and infrared gas analyzer, Naturwissenschaften 78 (1991) 168–170.
[41] Govindjee, C. Xu, J.J.S. van Rensen, On the requirement of bound bicarbonate for photosystem II activity, Z. Naturforsch. 52 (1997) 24–32.
[42] A. Stemler, Absence of a formate-induced release of bicarbonate from photosystem 2, Plant Physiol. 91 (1989) 287–290.
[43] P.A. Jursinic, A. Stemler, High-rates of photosystem II electron flow occur in maize thylakoids when the high-affinity binding-site for bicarbonate is empty of all monovalent anions or has bicarbonate bound, Biochim. Biophys. Acta 1098 (1992) 359–367.
[44] D. Shevela, V. Klimov, J. Messinger, Formate-induced release of carbon dioxide/hydrogencarbonate from photosystem II, in: J.F. Allen, E. Gantt, J.H. Golbeck, B. Osmond (Eds.), 14th International Congress on Photosynthesis Springer, Glasgow, 2008, pp. 497–501.
[45] D.A. Berthold, G.T. Babcock, C.F. Yocum, A highly resolved, oxygen-evolving photosystem II preparation from spinach thylakoid membranes, FEBS Lett. 134 (1981) 231–234.
[46] T. Kuwabara, N. Murata, Inactivation of photosynthetic oxygen evolution and concomitant release of three polypeptides in the photosystem II particles of spinach chloroplasts, Plant Cell Physiol. 23 (1982) 533–539.
[47] J. Messinger, G. Seaton, T. Wydrzynski, U. Wacker, G. Renger, S-3 state of the water oxidase in photosystem II, Biochemistry 36 (1997) 6862–6873.
[48] J. Messinger, J.H.A. Nugent, M.C.W. Evans, Detection of an EPR multiline signal for the S_0* state in photosystem II, Biochemistry 36 (1997) 11055–11060.
[49] C.F. Yocum, C.T. Yerkes, R.R. Sharp, R.E. Blankenship, G.T. Babcock, Stoichiometry, inhibitor sensitivity, and organization of manganese associated with photosynthetic oxygen evolution, Proc. Natl. Acad. Sci. U. S. A. 78 (1981) 7507–7511.
[50] J. Messinger, U. Wacker, G. Renger, Unusual low reactivity of the water oxidase in the redox state S_3 toward exogenous reductants. Analysis of the NH_2OH and NH_2NH_2 induced modifications of flash induced oxygen evolution in isolated spinach thylakoids, Biochemistry 30 (1991) 7852–7862.
[51] L. Konermann, J. Messinger, W. Hillier, Mass spectrometry based methods for studying kinetics and dynamics in biological systems, in: T.J. Aartsma, J. Matysik (Eds.), Biophysical Techniques in Photosynthesis (Volume II), vol. 26, Springer, Dordrecht, 2008, pp. 167–190.
[52] J. Messinger, M. Badger, T. Wydrzynski, Detection of one slowly exchanging substrate water molecule in the S_3 state of photosystem II, Proc. Natl. Acad. Sci. U. S. A. 92 (1995) 3209–3213.
[53] M.S. Khristin, L.K. Ignatova, N.N. Rudenko, B.N. Ivanov, V.V. Klimov, Photosystem II associated carbonic anhydrase activity in higher plants is situated in core complex, FEBS Lett. 577 (2004) 305–308.

[54] A. Stemler, P. Jursinic, The effects of carbonic-anhydrase inhibitors formate, bicarbonate, acetazolamide, and imidazole on photosystem II in maize chloroplasts, Arch. Biochem. Biophys. 221 (1983) 227–237.
[55] Y.N. Kozlov, S.K. Zharmukhamedov, K.G. Tikhonov, J. Dasgupta, A.A. Kazakova, G.C. Dismukes, V.V. Klimov, Oxidation potentials and electron donation to photosystem II of manganese complexes containing bicarbonate and carboxylate ligands, Phys. Chem. Chem. Phys. 6 (2004) 4905–4911.
[56] H. Kretschmann, H.T. Witt, Chemical reduction of the water splitting enzyme system of photosynthesis and its light-induced reoxidation characterized by optical and mass spectrometric measurements: a basis for the estimation of the states of the redox active manganese and of water in the quaternary oxygen evolving S-state cycle, Biochim. Biophys. Acta 1144 (1993) 331–345.
[57] A. Panja, N. Shaikh, S. Gupta, R.J. Butcher, P. Banerjee, New mononuclear manganese(III) complexes with hexadentate (N_4O_2) Schiff base ligands: synthesis, crystal structures, electrochemistry, and electron-transfer reactivity towards hydroxylamine, Eur. J. Inorg. Chem. (2003) 1540–1547.
[58] I.A. Salem, A kinetic-study of the homogeneous oxidation of hydroxylamine by manganese(III)-bis(salicylaldimine) complexes, Transition Met. Chem. 20 (1995) 312–315.
[59] G. Ulas, G. Olack, G.W. Brudvig, Evidence against bicarbonate bound in the O_2-evolving complex of photosystem II, Biochemistry 47 (2008) 3073–3075.
[60] V. Petrouleas, Y. Deligiannakis, B.A. Diner, Binding of carboxylate anions at the nonheme Fe^{II} of PSII. 2. Competition with bicarbonate and effects on the Q_A/Q_B electron-transfer rate, Biochim. Biophys. Acta 1188 (1994) 271–277.
[61] B.A. Diner, V. Petrouleas, Formation by NO of nitrosyl adducts of redox components of the photosystem II reaction center. 2. Evidence that HCO_3^-/CO_2 binds to the acceptor-side non-heme iron, Biochim. Biophys. Acta 1015 (1990) 141–149.
[62] C. Aoyama, H. Suzuki, M. Sugiura, T. Noguchi, Flash-induced FTIR difference spectroscopy shows no evidence for the structural coupling of bicarbonate to the oxygen-evolving Mn cluster in photosystem II, Biochemistry 47 (2008) 2760–2765.
[63] O.V. Pobeguts, T.N. Smolova, O.M. Zastrizhnaya, V.V. Klimov, Protective effect of bicarbonate against extraction of the extrinsic proteins of the water-oxidizing complex from Photosystem II membrane fragments, Biochim. Biophys. Acta 1767 (2007) 624–632.
[64] V.V. Klimov, S.V. Baranov, S.I. Allakhverdiev, Bicarbonate protects the donor side of photosystem II against photoinhibition and thermoinactivation, FEBS Lett. 418 (1997) 243–246.
[65] A. Villarejo, T. Shutova, O. Moskvin, M. Forssen, V.V. Klimov, G. Samuelsson, A photosystem II-associated carbonic anhydrase regulates the efficiency of photosynthetic oxygen evolution, EMBO J. 21 (2002) 1930–1938.
[66] M. Moubarak-Milad, A. Stemler, Oxidation-reduction potential dependence of photosystem II carbonic-anhydrase in maize thylakoids, Biochemistry 33 (1994) 4432–4438.
[67] I.L. McConnell, M.R. Badger, T. Wydrzynski, W. Hillier, A quantitative assessment of the carbonic anhydrase activity in photosystem II, Biochim. Biophys. Acta 1767 (2007) 639–647.
[68] Y.K. Lu, A.J. Stemler, Differing responses of the two fonns of photosystem II carbonic anhydrase to chloride, cations, and pH, Biochim. Biophys. Acta 1767 (2007) 633–638.
[69] J. Karlsson, A.K. Clarke, Z.Y. Chen, S.Y. Hugghins, Y.I. Park, H.D. Husic, J.V. Moroney, G. Samuelsson, A novel alpha-type carbonic anhydrase associated with the thylakoid membrane in *Chlamydomonas reinhardtii* is required for growth at ambient CO_2, EMBO J. 17 (1998) 1208–1216.
[70] T. Shutova, H. Kenneweg, J. Buchta, J. Nikitina, V. Terentyev, S. Chernyshov, B. Andersson, S.I. Allakhverdiev, V.V. Klimov, H. Dau, W. Junge, G. Samuelsson, The photosystem II-associated Cah3 in *Chlamydomonas* enhances the O_2 evolution rate by proton removal, EMBO J. 27 (2008) 782–791.
[71] S.V. Baranov, G.M. Ananyev, V.V. Klimov, G.C. Dismukes, Bicarbonate accelerates assembly of the inorganic core of the water-oxidizing complex in manganese depleted photosystem II: a proposed biogeochemical role for atmospheric carbon dioxide in oxygenic photosynthesis, Biochemistry 39 (2000) 6060–6065.
[72] S.V. Baranov, A.M. Tyryshkin, D. Katz, G.C. Dismukes, G.M. Ananyev, V.V. Klimov, Bicarbonate is a native cofactor for assembly of the manganese cluster of the photosynthetic water oxidizing complex. Kinetics of reconstitution of O_2 evolution by photoactivation, Biochemistry 43 (2004) 2070–2079.
[73] G.C. Dismukes, R.E. Blankenship, The origin and evolution of photosynthetic oxygen production, in: T. Wydrzynski, K. Satoh (Eds.), Photosystem II. The Light-driven Water:Plastoquinone Oxidoreductase, Springer, Dordrecht, 2005, pp. 683–695.
[74] G.C. Dismukes, V.V. Klimov, S.V. Baranov, Y.N. Kozlov, J. DasGupta, A. Tyryshkin, The origin of atmospheric oxygen on earth: the innovation of oxygenic photosynthesis, Proc. Natl. Acad. Sci. U. S. A. 98 (2001) 2170–2175.
[75] P.A. Castelfranco, Y.K. Lu, A.J. Stemler, Hypothesis: the peroxydicarbonic acid cycle in photosynthetic oxygen evolution, Photosynth. Res. 94 (2007) 235–246.
[76] R. Radmer, O. Ollinger, Isotopic composition of photosynthetic O_2 flash yields in the presence of $H_2^{18}O$ and $HC^{18}O_3^-$, FEBS Lett. 110 (1980) 57–61.
[77] V.V. Klimov, S.I. Allakhverdiev, Y. Nishiyama, A.A. Khorobrykh, N. Murata, Stabilization of the oxygen-evolving complex of photosystem II by bicarbonate and glycinebetaine in thylakoid and subthylakoid preparations, Funct. Plant Biol. 30 (2003) 797–803.
[78] N.E. Good, Carbon dioxide and the hill reaction, Plant Physiol. 38 (1963) 298–304.